

ARTICLE

Open Access

# Role of FGFR2b expression and signaling in keratinocyte differentiation: sequential involvement of PKC $\delta$ and PKC $\alpha$

Benedetta Rosato<sup>1</sup>, Danilo Ranieri<sup>1</sup>, Monica Nanni<sup>1</sup>, Maria Rosaria Torrisi<sup>1,2</sup> and Francesca Belleudi<sup>1</sup>

## Abstract

The tumor suppressor epithelial isoform of the fibroblast growth factor receptor 2 (FGFR2b) induces human keratinocyte early differentiation. Moreover, protein kinases C (PKCs) are known to regulate the differentiation program in several cellular contexts, including keratinocytes. Therefore, in this paper we propose to clarify if FGFR2b could play a role also in the late steps of keratinocyte differentiation and to assess if this receptor-induced process would sequentially involve PKC $\delta$  and PKC $\alpha$  isoforms. Immunofluorescence, biochemical, and molecular approaches, performed on 2D cultures or 3D organotypic rafts of human keratinocytes overexpressing FGFR2b by stable transduction, showed that receptor signaling induced the precocious onset and an accelerated progression of keratinocyte differentiation, indicating that FGFR2b is a crucial regulator of the entire program of keratinocyte differentiation. In addition, the use of specific inhibitors and gene silencing approaches through specific siRNA demonstrated that PKC $\delta$  controls the onset of FGFR2b-triggered differentiation, while PKC $\alpha$  plays a role restricted to the terminal stages of the process. Molecular analysis revealed that the two PKC isoforms sequentially act via induction of KLF4 and DLX3, two transcription factors linked by negative loops to p63, suggesting that p63 would represent the hub molecule at the crossroad of an intricate signaling network downstream FGFR2b, involving multiple PKC-induced transcription factors.

## Introduction

The family of fibroblast growth factor receptors (FGFRs) includes four transmembrane receptor tyrosine kinases (FGFR1–4) involved in the regulation of crucial biological processes, such as proliferation, migration, survival, and differentiation<sup>1,2</sup>. Alternative splicing of the extracellular IgIII loop in FGFR1-3 generates epithelial FGFRb and mesenchymal FGFRc isoforms, determining ligand specificity<sup>1</sup>. Deregulation of the expression and signaling of FGFRs is well known to play oncogenic

roles<sup>3,4</sup>. In the case of FGFR2, altered isoform switching and aberrant expression of the mesenchymal FGFR2c isoform in epithelial cells induce epithelial-mesenchymal transition (EMT)<sup>5,6</sup> and are involved in cancerogenesis<sup>7,8</sup>, while the epithelial FGFR2b variant appears to exert tumor suppressive functions<sup>9,10</sup>.

In agreement with the knowledge of the key role played by FGFR2b in the regulation of skin homeostasis<sup>11–13</sup>, studies from our group have demonstrated that FGFR2b is up-regulated in epidermal suprabasal layers<sup>14</sup> and is able to induce early differentiation in normal human keratinocytes<sup>15</sup>. We have also suggested that FGFR2b exerts its differentiative function via the repression of p63<sup>16</sup>, a transcription factor whose down-modulation represents the main molecular mechanism known to drive

Correspondence: Francesca Belleudi ([francesca.belleudi@uniroma1.it](mailto:francesca.belleudi@uniroma1.it))

<sup>1</sup>Department of Clinical and Molecular Medicine, Laboratory affiliated to Istituto Pasteur Italia—Fondazione Cenci Bolognetti, Sapienza University of Rome, Roma, Italy

<sup>2</sup>S. Andrea University Hospital, Rome, Italy

These authors contributed equally: Benedetta Rosato, Danilo Ranieri.

These authors jointly supervised this work: Maria Rosaria Torrisi, Francesca Belleudi.

Edited by E Candi.

© The Author(s) 2018



**Open Access** This article is licensed under a Creative Commons Attribution 4.0 International License, which permits use, sharing, adaptation, distribution and reproduction in any medium or format, as long as you give appropriate credit to the original author(s) and the source, provide a link to the Creative Commons license, and indicate if changes were made. The images or other third party material in this article are included in the article's Creative Commons license, unless indicated otherwise in a credit line to the material. If material is not included in the article's Creative Commons license and your intended use is not permitted by statutory regulation or exceeds the permitted use, you will need to obtain permission directly from the copyright holder. To view a copy of this license, visit <http://creativecommons.org/licenses/by/4.0/>.

early differentiation of stratified epithelia<sup>17</sup>. Although the role of FGFR2b in early stages of keratinocyte differentiation has been deeply investigated, its involvement in the later steps of the process still remains debated<sup>18–20</sup> and to be clarified.

With the aim to analyze the possible signaling candidates for the regulation of FGFR2b-mediated early differentiation, we have previously demonstrated the involvement of the PI3K/AKT pathway<sup>15</sup>. However, the keratinocyte differentiation is a complex program implying several steps of coordinated molecular events driven by an intricate signaling network; therefore, to verify if additional pathways downstream FGFR2b could participate to such network, we focused our attention on protein kinases C (PKCs) and in particular to the PKC $\delta$  and PKC $\alpha$  isoforms. In fact, these signaling substrates are involved in FGFR2-mediated differentiation in the bone context<sup>21,22</sup> and it has been proposed that PKC $\delta$  and PKC $\alpha$  could regulate keratinocyte differentiation<sup>23</sup>, during which they appear to exert temporally and spatially distinct roles.

A function in the onset of keratinocyte differentiation has been proposed for PKC $\delta$ <sup>23–29</sup>, which is expressed starting from the basal layer of epidermis where, upon activation, causes hemidesmosomal disassembly and basal cell migration upward into the suprabasal layers<sup>30,31</sup>. At the level of transcriptional control, PKC $\delta$  induces the early differentiation marker desmoglein-1 (DSG1)<sup>26</sup>. Moreover, recent studies highlighted that PKC $\delta$ , through the induction of the transcription factor Kruppel-like factor 4 (KLF4), up-modulates p21 and the intermediate differentiation marker involucrin (INV)<sup>32</sup> triggering cell cycle arrest and differentiation, respectively<sup>28,29</sup>.

On the other hand, a role in epidermal late differentiation has been proposed for PKC $\alpha$ . In fact, PKC $\alpha$  expression is restricted to epidermal suprabasal layers<sup>23</sup> and its inhibition or depletion represses the expression of the late differentiation markers filaggrin (FIL) and loricrin (LOR)<sup>32</sup>, while the early/intermediate differentiation markers keratin 1 (K1), K10, and INV<sup>32</sup> appear substantially unaffected<sup>25,27,33–36</sup>. Distal-less homeobox 3 (DLX3) could be the molecular player acting downstream PKC $\alpha$  in keratinocyte differentiation:<sup>36</sup> this transcription factor is expressed in the suprabasal layers and is involved in the induction of FIL and LOR, as well as in the epidermal barrier formation<sup>37–39</sup>.

Based on these assumptions, here we propose to clarify if FGFR2b could play a general role in the control of the entire program of keratinocyte differentiation and to assess if the possible function of FGFR2b in the different steps of the process might be regulated by a signaling network sequentially involving PKC $\delta$  and PKC $\alpha$  isoforms and their respective downstream transcription factors.

## Results

### FGFR2b controls not only the early, but also the late steps of keratinocyte differentiation

Studies from our group have demonstrated that FGFR2b expression and activation promote keratinocyte early differentiation<sup>15,16</sup>. Here, in order to investigate if FGFR2b might also control the later stages of differentiation, we first analyzed the impact of the receptor signaling on the expression and distribution throughout the epidermal layers of two distinct markers of the most early or the most late differentiation steps: the early cytokeratin K1 and the terminal differentiation FIL. For this purpose we reproduced in vitro the keratinocyte differentiation program occurring in vivo, using 3D organotypic skin equivalents prepared with human HaCaT keratinocytes<sup>40</sup> stably transduced with pBp-FGFR2b retroviral constructs or with empty pBp vector as negative control<sup>6</sup>. In fact, through this model of receptor-overexpressing cells we are able to force the system toward the differentiated phenotype. The organotypic cultures were left untreated or stimulated with FGF7 as reported in Materials and methods section. Quantitative immunofluorescence analysis showed that, in pBp rafts, the K1 signal was visible in all suprabasal layers (Fig. 1a, left panels) and increased by FGF7 stimulation (Fig. 1a, left panels), as expected<sup>15</sup>. Interestingly, HaCaT pBp-FGFR2b rafts showed, besides the enhancement of K1 staining (Fig. 1a, left panels), its appearance already in the basal layer (Fig. 1a, left panels), suggesting the precocious onset of early differentiation. Parallel evaluation of FIL expression showed that, as expected<sup>32</sup>, its granular staining appeared confined in the uppermost layers of pBp skin equivalents (Fig. 1a, right panels) and it was significantly increased by FGF7 stimulation (Fig. 1a, right panels). In addition, FGFR2b overexpression induced a general enhancement of this staining and its appreciable appearance starting from lower layers of the rafts (Fig. 1a, right panels), suggesting an accelerated progression also throughout the terminal steps of differentiation. As previously reported<sup>41</sup>, the higher staining of the analyzed markers in pBp-FGFR2b untreated organotypic cultures respect to the corresponding unstimulated pBp rafts would be ascribed to the already acquired enhanced differentiated phenotype of the FGFR2b clones during their growth in complete medium before starvation. Our observations were also validated at molecular level by real time RT-PCR analysis, demonstrating that the expression of early (K10 and DSG1), intermediate (INV, transglutaminase-1: TGM1) and late differentiation marker (LOR) genes were significantly increased in response to FGF7 and particularly in cells overexpressing FGFR2b (Fig. 1b). Thus, FGFR2b and its signaling appear to play a positive role on the entire program of keratinocyte differentiation.

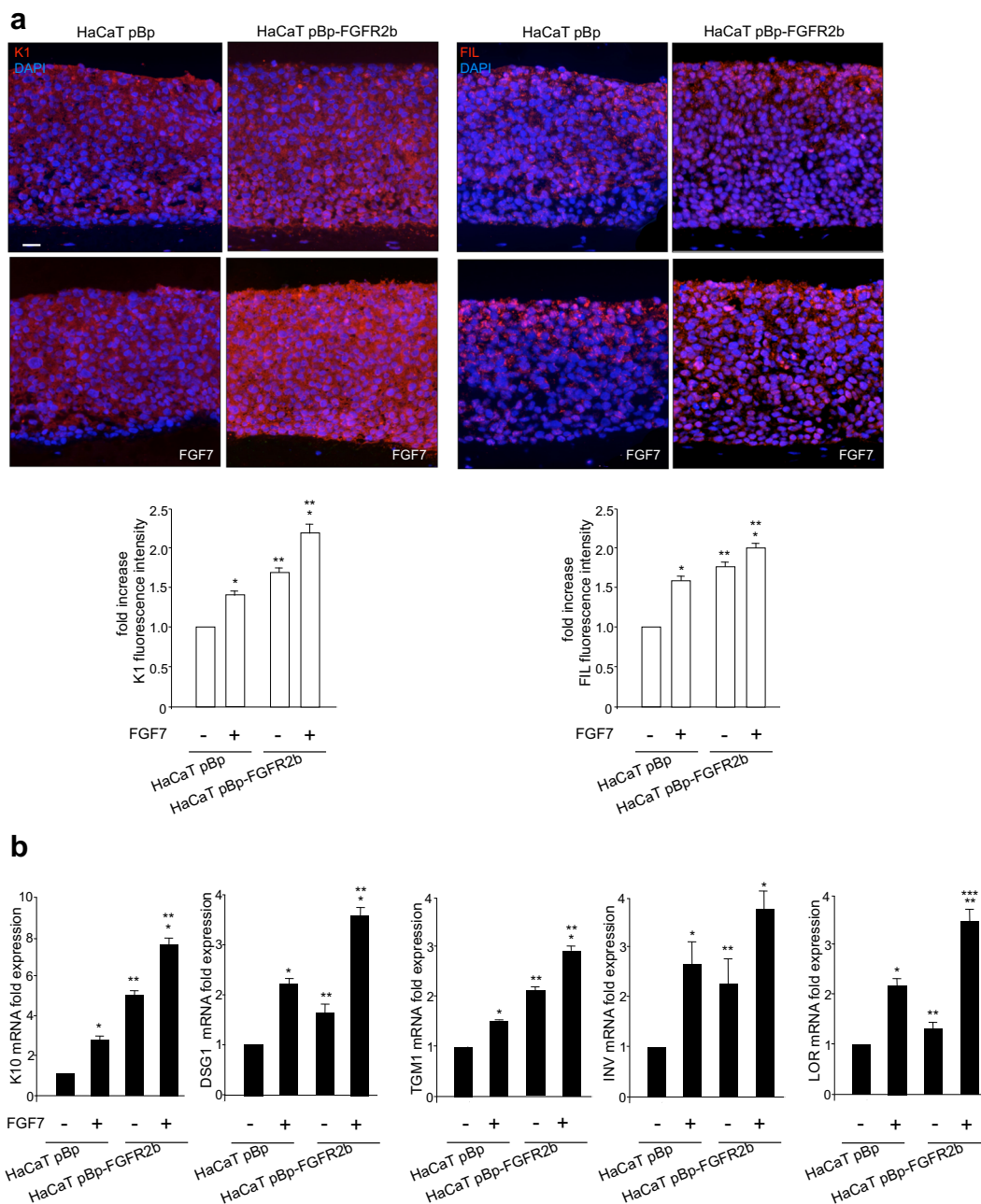


**Fig. 1** FGFR2b expression and signaling play a positive role on the entire program of keratinocyte differentiation. Organotypic skin equivalents of HaCaT pBp and pBp-FGFR2b clones, prepared as reported in Materials and methods section, were grown in complete medium and left untreated or stimulated with FGF7 for the last 4 days. **a** Quantitative immunofluorescence analysis shows that, in pBp rafts, K1 staining is visible in all suprabasal layers and it is increased by FGF7 stimulation. In HaCaT pBp-FGFR2b raft K1 staining is enhanced and detectable already in the basal layer. Parallel evaluation of FIL expression shows that its granular staining appears confined in the uppermost layers of pBp skin equivalents and it is significantly increased by FGF7 stimulation. FGFR2b overexpression induces a general enhancement of the staining and its appreciable appearance starting from lower layers of the rafts. Quantitative analysis of the fluorescence intensity was performed as described in Materials and methods and results sections are expressed as fold increase respect to pBp values  $\pm$  SE. Student's *t* test was performed and significance levels have been defined as  $p < 0.05$ : \* $p < 0.0001$  vs the corresponding FGF7-unstimulated cells; \*\* $p < 0.0001$  vs the corresponding pBp cells. Bar: 25  $\mu$ m. **b** Real time RT-PCR analysis shows that mRNA expression of the early (K10 and DSG1), intermediate (TGM1 and INV) and late differentiation (LOR) markers are significantly increased upon FGF7 stimulation, particularly in pBp-FGFR2b rafts. Results are expressed as mean values  $\pm$  SD. Student's *t* test was performed and significance levels have been defined as  $p < 0.05$ : \* $p < 0.05$ , and \*\*\* $p < 0.005$  vs the corresponding FGF7-unstimulated cells; \*\* $p < 0.05$  vs the corresponding pBp cells

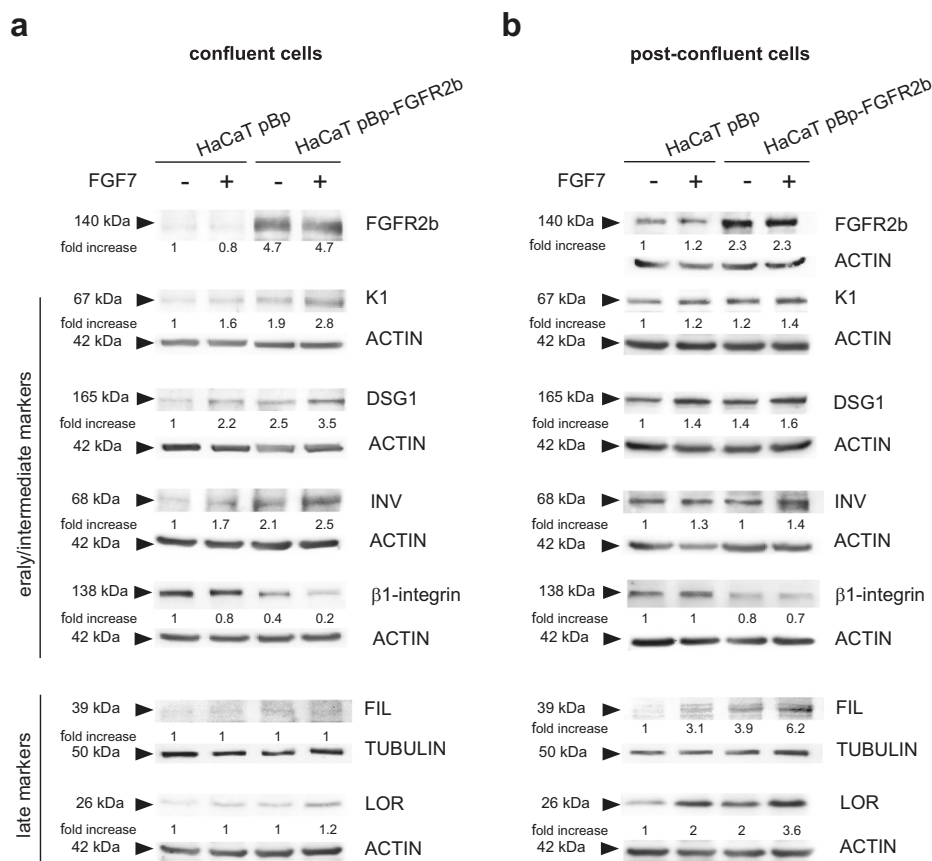


**Fig. 2** FGFR2b has a sequential role in distinct steps of the keratinocyte differentiation. HaCaT pBp and HaCaT pBp-FGFR2b clones grown up to confluence or post-confluence were left untreated or stimulated with FGF7 as reported in Materials and methods section. **a** Western blot analysis shows that in confluent conditions the levels of K1, DSG1, and INV are increased upon FGF7 stimulation particularly in pBp-FGFR2b cells, while no appreciable levels of FIL and LOR are visible in these cells. In addition, the expression of  $\beta$ 1-integrin appears strongly decreased in HaCaT pBp-FGFR2b in response to ligand stimulation. **b** In post-confluence conditions all the early/intermediate differentiation markers appear increased making their FGF7-induced modulation less evident compared to the corresponding confluent cells. In contrast, FIL and LOR are detectable and they appear up-regulated in response to FGF7 stimulation, particularly in cells overexpressing FGFR2b. The equal loading was assessed with anti-ACTIN and anti-TUBULIN antibodies. For densitometric analysis the values from a representative of three independent experiments are reported

In order to analyze in detail this role, we “dissected” in vitro the process using HaCaT pBp and HaCaT pBp-FGFR2b cultures grown until confluence, the step that precedes the shift from the basal to suprabasal layer, or up to post-confluence, the step that mimics the late differentiation and stratification<sup>40</sup>. Cells were then left untreated or stimulated with FGF7, as reported in Materials and methods section, and Western blot analysis was performed to estimate the expression of a wide selection of differentiation markers. Results showed that, in confluent conditions, a clear up-regulation of the early differentiation markers K1 and DSG1 and of the intermediate differentiation marker INV was induced by FGF7, particularly in pBp-FGFR2b cells (Fig. 2a). In addition, an opposite behavior was observed for the basal marker  $\beta$ 1-integrin<sup>42</sup>, whose expression appeared strongly decreased in HaCaT pBp-FGFR2b in response to ligand

stimulation (Fig. 2a). Finally, in agreement with their similarities with basal/differentiating keratinocytes, no appreciable levels of the late differentiation marker FIL and LOR were found in all confluent HaCaT clones (Fig. 2a). On the other hand, the shift to post-confluence strongly increased the expression of all the differentiation markers (Fig. 2b), making their FGF7-induced modulation less evident compared to the corresponding confluent cells (Fig. 2b). Moreover, as already observed in 3D organotypic cultures, pBp-FGFR2b cells showed a higher differentiated phenotype compared to pBp cultures also in the absence of FGF7 stimulation, which can be ascribed to the enhanced differentiation acquired during the growth in complete medium before starvation. The observed progressive modulation in response to FGF7 of early/intermediate and LORs in confluent and post-confluent cultures of HaCaT clones, respectively, was also

confirmed at the mRNA transcript level (Supplementary Figure S1).

### **PKC $\delta$ and PKC $\alpha$ signaling play sequential roles in FGFR2b-triggered keratinocyte differentiation**

Searching for the possible downstream candidates that could be alternatively involved in FGFR2b-mediated early or late differentiation, we focused our attention on PKC $\delta$  and PKC $\alpha$  isoforms, since they have been proposed to exert distinct roles in keratinocyte differentiation<sup>23</sup>.

Since PKC $\delta$  isoform has been proposed to be specifically implicated in the onset of the process<sup>23–29</sup>, we first investigated its contribution in FGFR2b-induced early differentiation taking advantage of the specific inhibitor rottlerin (PKC $\delta$ i), previously used to demonstrate the involvement of PKC $\delta$  in FGF/FGFR signaling pathways<sup>21</sup>, as well as in FGFR2b-triggered autophagy<sup>43</sup>. The inhibitor efficiency was confirmed testing its ability to decrease the basal, as well as the FGF7-induced, phosphorylation of PKC $\delta$  at the autophosphorylation site Serine 645<sup>44</sup> (Fig. 3a, left panel), but not that of PKC $\alpha$  at the autophosphorylation site Serine 657<sup>45</sup> (Fig. 3a, left panel). Then we analyzed the impact of this inhibitor on the modulation of early/intermediate differentiation markers induced by FGFR2b and its signaling in confluent cultures. Western blot analysis clearly showed that PKC $\delta$ i exerted a strong repressive effect on the K1, DSG1, and INV increase induced by FGF7, which was particularly evident in FGFR2b overexpressing clones (Fig. 3a, right panel). Indeed, in agreement with the proposed general role of PKC $\delta$  in keratinocyte early differentiation<sup>23</sup>, this inhibitory effect, even if less pronounced, was also detectable in cells not stimulated with FGF7 (Fig. 3a, right panel). However, to exclude the possibility of the establishment of an autocrine signaling due to endogenous production of FGF7, which could explain the phenotype displayed by unstimulated FGFR2b clones, we performed real time RT-PCR analysis: FGF7 mRNA was undetectable in both HaCaT clones also after PKC signaling shut-off (data not shown). To unequivocally demonstrate the role of PKC $\delta$  on early differentiation, we performed its specific depletion by siRNA transfection. To this aim, HaCaT clones were transfected with PKC $\delta$  siRNA or with an unrelated siRNA as control. The efficiency of protein depletion was verified through Western blot analysis (Fig. 3b, left panel). Transfected cells were grown until confluence and left untreated or stimulated with FGF7 as above. Western blot analysis showed that PKC $\delta$  silencing strongly counteracted the increase of K1, DSG1, and INV in response to FGF7 (Fig. 3b, right panel). In addition, similarly to what observed after the pharmacological inhibition, PKC $\delta$  depletion appeared to slightly affect also the basal level of the markers (Fig. 3b, right panel), confirming its general role in the control of early differentiation.

These findings were also validated at the mRNA transcript level by real time RT-PCR analysis, confirming that, in both HaCaT pBp and pBp-FGFR2b confluent cultures, the block of PKC $\delta$  activity by PKC $\delta$ i (Fig. 3c) or protein depletion by specific siRNA (Fig. 3d) strongly decreased FGF7-induced, as well as basal expression, of K10, DSG1, and INV. The results obtained were strengthened by quantitative immunofluorescence analysis (Supplementary Figure S2, left and right panels), in which we introduced also the inhibitor of AKT (AKTi)<sup>15,43,46</sup>, in order to interfere with the additional FGFR2b downstream pathway previously identified by us as involved in keratinocyte early differentiation<sup>15</sup>, or the MEK1/2 inhibitor (MEK1/2i), as negative control, since we have recently observed that this pathway did not appear to be involved in the process (Nanni et al., manuscript in preparation). In fact, while the role played by AKT signaling appears to be restricted to some aspects of FGFR2b-induced early steps of the process, PKC $\delta$  emerges as hub signaling downstream FGFR2b regulating the entire early differentiation.

Because PKC $\alpha$  isoform has been proposed to be a signaling substrate crucial for the later steps of keratinocyte differentiation<sup>23,25,27,33–36</sup>, we investigated its possible contribution in FGFR2b-induced terminal steps of the process. To this aim the effects of PKC $\alpha$  inhibition were analyzed in post-confluent cultures of HaCaT clones using the specific inhibitor Go6976 (PKC $\alpha$ i)<sup>36</sup>. The efficiency of PKC $\alpha$ i was assessed by Western blot analysis, performed in both HaCaT pBp and pBp-FGFR2b cultures, showing a decrease of the basal, as well as the FGF7-induced PKC $\alpha$  phosphorylation at the autophosphorylation site Serine 657<sup>45</sup> (Fig. 4a, left panel), but not that of PKC $\delta$  at the autophosphorylation site Serine 645<sup>44</sup> (Fig. 4a, left panel). Then we investigated if PKC $\alpha$ i could affect FGFR2b-induced differentiation. Western blot analysis highlighted that PKC $\alpha$ i did not interfere with the expression of the early differentiation marker K1 (Fig. 4a, right panel), but it displayed a strong repressive effect on the FGF7-induced up-modulation of the late differentiation markers LOR and FIL (Fig. 4a, right panel). Moreover, also the basal level of LOR and FIL markers expressed in cells not stimulated with FGF7 appeared weakly dampened by PKC $\alpha$ i, confirming the general role of PKC $\alpha$  in keratinocyte differentiation<sup>23</sup>. Similar results were obtained by specific siRNA approaches. The efficiency of protein depletion was first confirmed by Western blot analysis (Fig. 4b, left panel). Then, the effects of PKC $\alpha$  silencing showed repression of the late differentiation markers LOR and FIL (Fig. 4b, right panel), but not of the early differentiation marker K1 (Fig. 4b, right panel) in both pBp and pBp-FGFR2b clones. The inhibitory effect of either PKC $\alpha$  pharmacological inhibition (Fig. 4c) and protein depletion (Fig. 4d) was also confirmed at the mRNA transcript level by real time RT-PCR

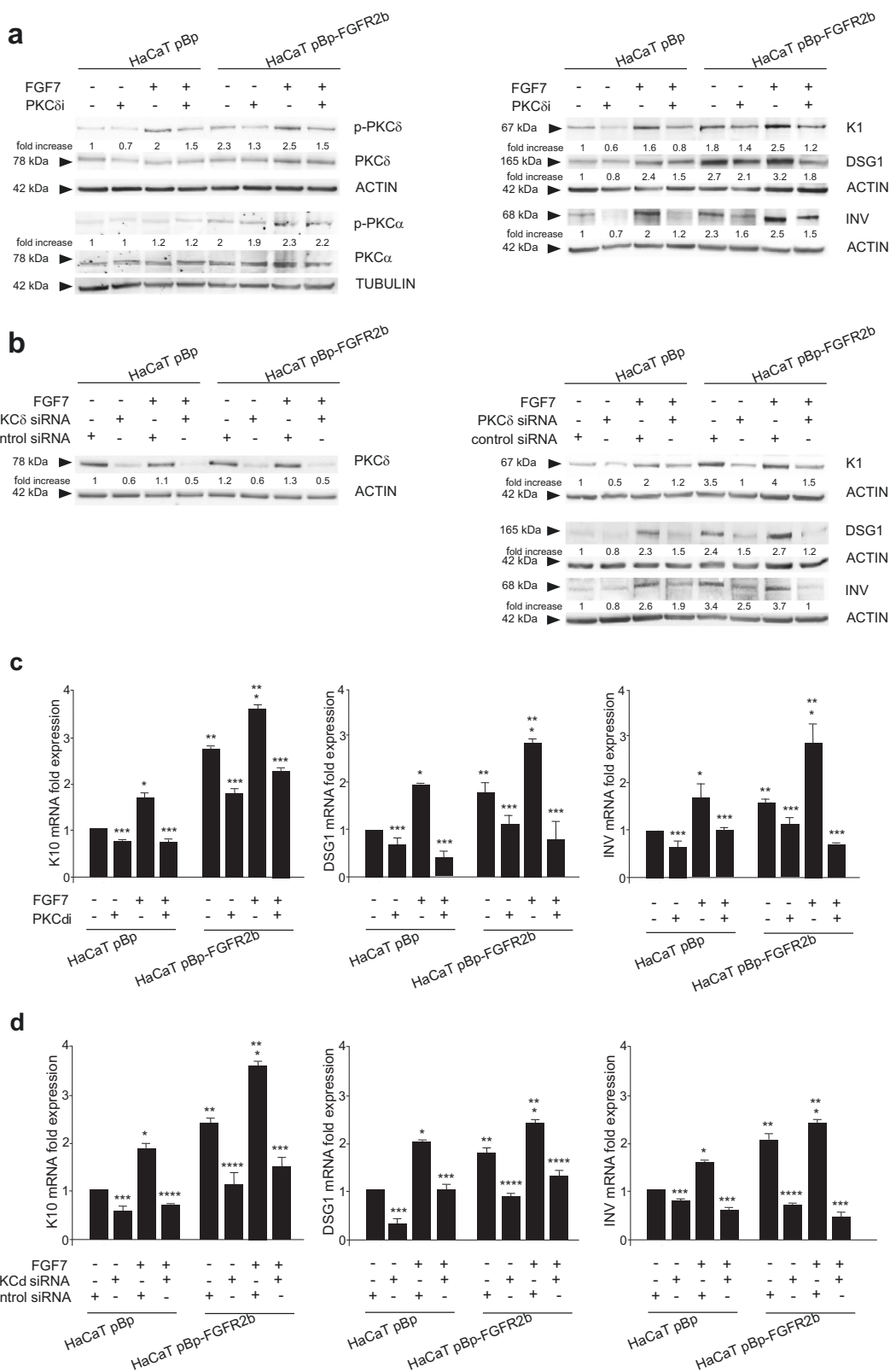


**Fig. 3** (See legend on next page.)

(see figure on previous page)

**Fig. 3 PKC $\delta$  controls the onset of FGFR2b-triggered keratinocyte differentiation.** Confluent HaCaT pBp and HaCaT pBp-FGFR2b clones were left untreated or stimulated with FGF7 in presence or not of the PKC $\delta$  inhibitor as reported in Materials and methods section (**a, c**). Alternatively, HaCaT clones were transfected with PKC $\delta$  siRNA or with an unrelated siRNA as control, and then left untreated or stimulated with FGF7 (**b, d**). **a** Western blot analysis confirms that PKC $\delta$  inhibitor interferes with the basal, as well as the FGF7-induced, phosphorylation of PKC $\delta$  at its autophosphorylation site Ser645 but not with that of PKC $\alpha$  at its autophosphorylation site Ser657 (left panel). PKC $\delta$  inhibition induces a repressive effect on the K1, DSG1, and INV increase induced by FGF7, which is particularly evident in FGFR2b overexpressing clones (right panel). **b** Western blot analysis confirms that PKC $\delta$  silencing specifically dampened the basal, as well as the FGF7-induced, PKC $\delta$  protein level but not that of PKC $\alpha$  (left panel). PKC $\delta$  silencing also strongly counteracts the increase of K1, DSG1, and INV in response to FGF7 (right panel). The equal loading was assessed with anti-PKC $\delta$  or anti-PKC $\alpha$  and anti-ACTIN or anti-TUBULIN antibodies. For densitometric analysis the values from a representative of three independent experiments are reported. **c, d** Real time RT-PCR analysis confirms that PKC $\delta$  inhibition (**c**) or depletion (**d**) decreases FGF7-induced, as well as basal mRNA transcript levels, of K10 DSG1 and INV. Results are expressed as mean values  $\pm$  SD. Student's *t* test was performed and significance levels have been defined as above: **c** \**p* < 0.05 vs the corresponding FGF7-unstimulated cells; \*\**p* < 0.05 vs the corresponding pBp cells; \*\*\**p* < 0.05 vs the corresponding PKC $\delta$  inhibitor-untreated cells; **d** \**p* < 0.05 vs the corresponding FGF7-unstimulated cells; \*\**p* < 0.05 vs the corresponding pBp cells; \*\*\**p* < 0.05 and \*\*\*\**p* < 0.005 vs the corresponding control siRNA cells

analysis. Thus, also PKC $\alpha$  appears a pivotal player in FGFR2b-triggered keratinocyte differentiation; however, differently from PKC $\delta$ , its role appears to be specifically restricted to the late stages of the process.

Then, in order to analyze the effect of PKC $\delta$  inhibition on the ability of keratinocytes to progress throughout the entire differentiation program and stratify in response to FGFR2b activation, we again took advantage of the use of the more complete model of organotypic cultures. HaCaT pBp and HaCaT pBp-FGFR2b rafts were lifted to air-liquid interface in the presence or not of PKC $\delta$ i and finally stimulated with FGF7, as above. Quantitative immunofluorescence analysis showed that the K1 and FIL staining, visible in both HaCaT pBp and HaCaT pBp-FGFR2b rafts stimulated with FGF7 (Fig. 5a, upper panels), appeared overall dampened by the presence of PKC $\delta$ i, suggesting that the entire differentiation process induced by FGFR2b signaling was arrested by the sustained inhibition of PKC $\delta$  (Fig. 5a, upper panels). In addition, the immunostaining of K5 revealed that the canonical distribution in the basal layer of this undifferentiated/proliferating cell marker<sup>32</sup>, visible in pBp control rafts (Fig. 5a, lower panels), disappeared in pBp-FGFR2b skin equivalents (Fig. 5a, lower panels), confirming the precocious onset of differentiation. However, in the presence of PKC $\delta$ i, K5 staining appeared recovered and distributed all over the rafts (Fig. 5a, lower panels). Moreover, the parallel evaluation of Ki67 staining in both pBp and pBp-FGFR2b rafts stimulated with FGF7 revealed few positive cells distributed in the basal layer (Fig. 5a, lower panels); the presence of some stained cells also in the suprabasal layers (Fig. 5a, lower panels) is in agreement with the previously described ability of FGF7 to also sustain the residual proliferative activity of suprabasal keratinocytes<sup>14</sup>. More interestingly, in pBp-FGFR2b raft grown in the presence of PKC $\delta$ i, several cells intensely stained for Ki67 marker appeared homogeneously distributed in all the layers (Fig. 5a, lower panels), suggesting

sustained cell proliferation. These findings strongly indicated that, as a consequence of PKC $\delta$  signaling shut-off, keratinocytes are defective in the ability to undergo the differentiation program maintaining a basal/proliferative phenotype. Real time RT-PCR analysis confirmed that the expression of both early and LORs was significantly repressed by PKC $\delta$ i (Fig. 5b). Finally, the quantitative evaluation of the raft thickness revealed that, in pBp and pBp-FGFR2b skin equivalents, the layers were significantly reduced by PKC $\delta$ i (Fig. 5c), further indicating that inhibition of PKC $\delta$  induces impairment of all steps of FGFR2b-triggered differentiation, which in turn results in defective stratification.

#### The transcription factors KLF4 and DLX3, acting downstream PKC $\delta$ and PKC $\alpha$ respectively, are sequentially up-regulated by FGFR2b signaling

Since it has been recently proposed that PKC $\delta$  and PKC $\alpha$  control the expression of several genes via the induction of KLF4<sup>28,29</sup> and DLX3<sup>36</sup> respectively, we decided to investigate the possible involvement of these transcription factors in FGFR2b-triggered keratinocyte differentiation. The topic was particularly appealing, since they have been proposed to be involved in an intricate network of loops with  $\Delta$ Np63<sup>47-49</sup>, the transcription factor whose down-modulation represents the main molecular mechanism known to drive differentiation of stratified epithelia<sup>17</sup>. Indeed, we have already described a link between FGFR2b and p63<sup>16</sup>, but the molecular mechanism underlying this interplay remains to be still clarified. To this aim, we performed Real Time RT-PCR analysis on HaCaT pBp and pBp-FGFR2b 3D organotypic rafts, checking for the transcript levels of KLF4 and DLX3 and comparing them with that of p63. The results showed a significant increase of both KLF4 and DLX3 and an opposite decrease of p63 in response to FGF7 stimulation (Fig. 6a), which were more evident in the rafts overexpressing FGFR2b (Fig. 6a).

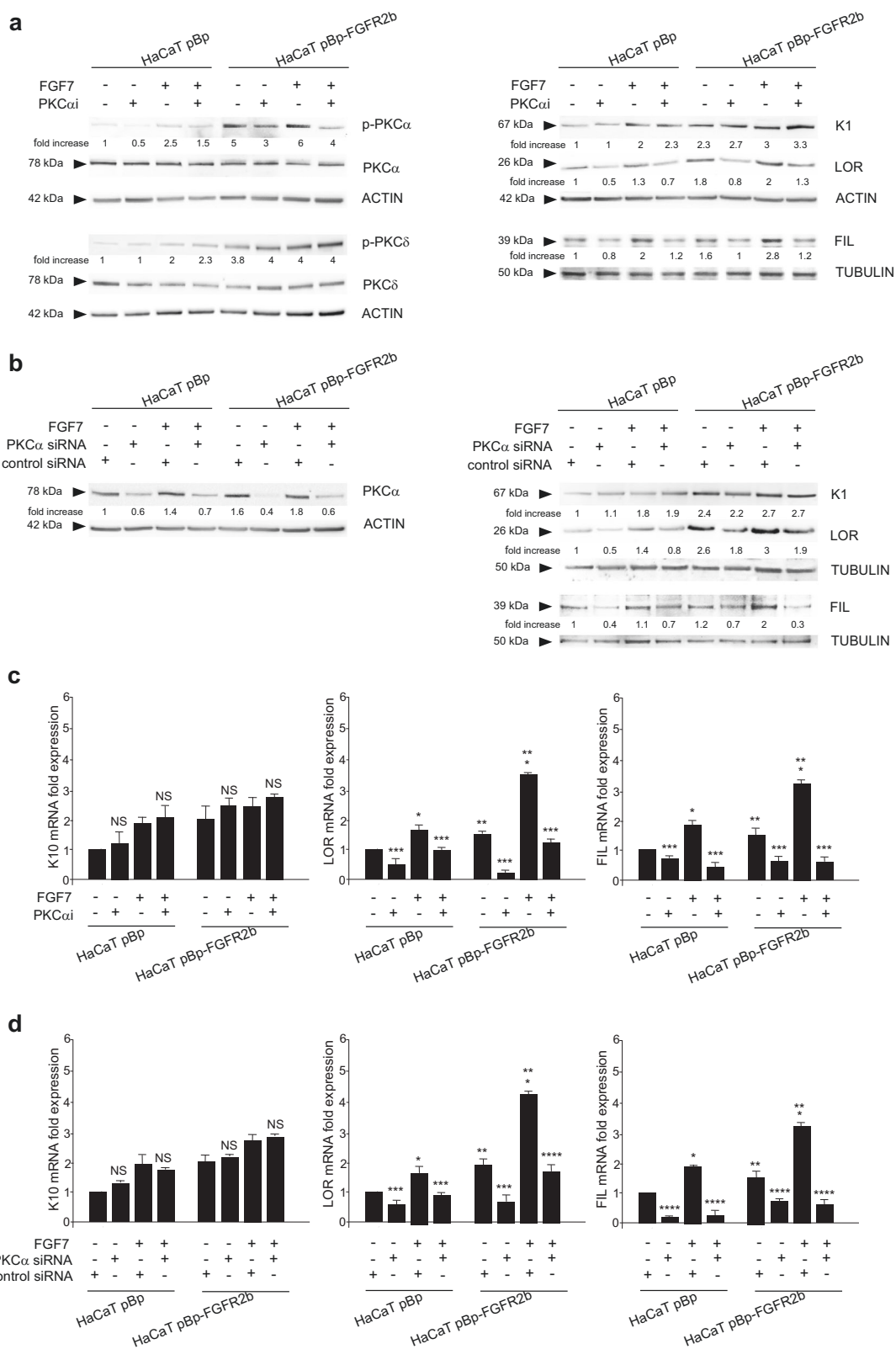


**Fig. 4** (See legend on next page.)



(see figure on previous page)

**Fig. 4 PKC $\alpha$  is required for FGFR2b-induced terminal stages of keratinocyte differentiation.** Post-confluent HaCaT pBp and HaCaT pBp-FGFR2b cells were left untreated or stimulated with FGF7 in presence or not of the PKC $\alpha$  inhibitor as reported in Materials and methods section (**a, c**). Alternatively, HaCaT clones were transfected with PKC $\alpha$  siRNA or with an unrelated siRNA as control, transfected cells were grown until post-confluence and left untreated or stimulated with FGF7 as above (**b, d**). **a** Western blot analysis shows that PKC $\alpha$  inhibitor decreases the basal, as well as the FGF7-induced, PKC $\alpha$  phosphorylation, but not that of PKC $\delta$  phosphorylation (left panel). PKC $\alpha$  inhibitor does not interfere with the K1 expression, but it displays a repressive effect on the FGF7-induced up-modulation of LOR and FIL (right panel). **b** Western blot analysis confirms that PKC $\alpha$  silencing specifically dampened the basal, as well as the FGF7-induced, PKC $\alpha$  protein level but not that of PKC $\delta$  (left panel). PKC $\alpha$  silencing also strongly counteracts the increase of LOR and FIL but not that of K1 in response to FGF7 (right panel). The equal loading was assessed with anti-PKC $\delta$  or anti-PKC $\alpha$  and anti-ACTIN or anti-TUBULIN antibodies. For densitometric analysis the values from a representative of three independent experiments are reported. **c, d** Real time RT-PCR analysis confirms that PKC $\alpha$  inhibition (**c**) or depletion (**d**) decreases FGF7-induced, as well as basal mRNA transcript levels, of LOR and FIL but it does not affect K10 expression. Results are expressed as mean values  $\pm$  SD. Student's *t* test was performed and significance levels have been defined as above: \**p* < 0.05 vs the corresponding FGF7-unstimulated cells; \*\**p* < 0.05 vs the corresponding pBp cells; NS and \*\*\**p* < 0.05 vs the corresponding PKC $\alpha$  inhibitor-untreated cells; **d** \**p* < 0.05 vs the corresponding FGF7-unstimulated cells; \*\**p* < 0.05 vs the corresponding pBp cells; NS, \*\*\**p* < 0.05 and \*\*\*\**p* < 0.005 vs the corresponding control siRNA cells

Then, to verify if KLF4 and DLX3 up-regulation could display a sequential trend during FGFR2b-induced keratinocyte differentiation, we analyzed their possible modulation in confluent and post-confluent clones stimulated with FGF7 as above. The results showed that KLF4 up-regulation was mainly appreciable in confluent clones (Fig. 6b), while DLX3 induction was detectable only in post-confluent cultures (Fig. 6b). As expected, the induction of KLF4 in confluent cells as well as that of DLX3 in post-confluent cells were significantly counteracted by PKC $\delta$ i and PKC $\alpha$ i, respectively (Fig. 6b), further confirming the connection of each PKC signaling with the corresponding transcription factor. Moreover, similarly to what observed for KLF4 and consistently with its well-established role in FGFR2b-induced onset of differentiation<sup>15,16</sup>, p63 repression in response to FGF7 was more evident in confluent cells and impaired only by PKC $\delta$ i (Fig. 6b). Being p63 a direct negative regulator of KLF4 in normal human keratinocytes<sup>49</sup>, its strong repression observed in confluent cells may represent the molecular mechanism through which FGFR2b-triggered PKC $\delta$  signaling would induce KLF4 and consequently the onset of keratinocyte differentiation. These results suggest that the alternative induction of KLF4 and DLX3 in FGF7-stimulated confluent and post-confluent cells, respectively, might reflect the sequential activation of their upstream activators PKC $\delta$  and PKC $\alpha$  during the early and late steps of FGFR2b-induced differentiation.

## Discussion

Because of its hypothesized role as a tumor suppressor *in vitro* and *in vivo*<sup>9,10</sup>, forced modulation of FGFR2b could be a winning strategy to revert important aspects of the malignant phenotype in carcinoma cells, including loss of cell differentiation. However, in the physiological context of normal human keratinocytes, despite the numerous evidences emphasizing the role of FGFR2b in the enhancement of early differentiation, only few and

contrasting reports appear to suggest its possible involvement in the later stages of this process<sup>18–20</sup>. Therefore, here we first analyzed the impact of the receptor signaling on the induction of terminal differentiation in 3D organotypic rafts and 2D cultures of human keratinocytes engineered to stably overexpress FGFR2b. The results obtained clearly indicated that, particularly when FGFR2b is overexpressed, the receptor signaling not only induces a precocious onset of the early differentiation markers, but also enhances the expression and accelerates the appearance of the terminal markers. These findings strongly suggest a key role of FGFR2b in the regulation of the entire differentiation program.

Then, in order to analyze the signaling players downstream FGFR2b possibly involved in keratinocyte differentiation, we focused on PKC $\delta$  and PKC $\alpha$  isoforms, at the light of previous evidences showing their sequential role in the regulation of the different steps of the process<sup>23</sup>. To the aim to “dissect” *in vitro* the differentiation steps, cells were grown until confluence or up to post-confluence. Taking advantage of the use of specific substrate inhibitors and siRNA interference, we highlighted that PKC $\delta$  signaling appears to drive the early molecular events, while PKC $\alpha$  regulates the late ones, of FGFR2b-triggered keratinocyte differentiation. Given the role of PKC $\delta$  in the onset of the process, we used the organotypic cultures to analyze the impact of its inhibition on the ability of keratinocytes to terminally differentiate and stratify in response to ligand-mediated activation of FGFR2b: we demonstrated that PKC $\delta$  signaling shut-off was sufficient to block the entire differentiation program, inducing retention of undifferentiated/basal features and defective stratification. Interestingly, these rafts also maintained a sustained cell proliferation throughout all the layers that could be explained by the previously described ability of FGFR2b to not only promote the differentiation program<sup>15</sup>, but also sustain the residual proliferative activity of suprabasal, differentiating keratinocytes<sup>14</sup>. Overall, the

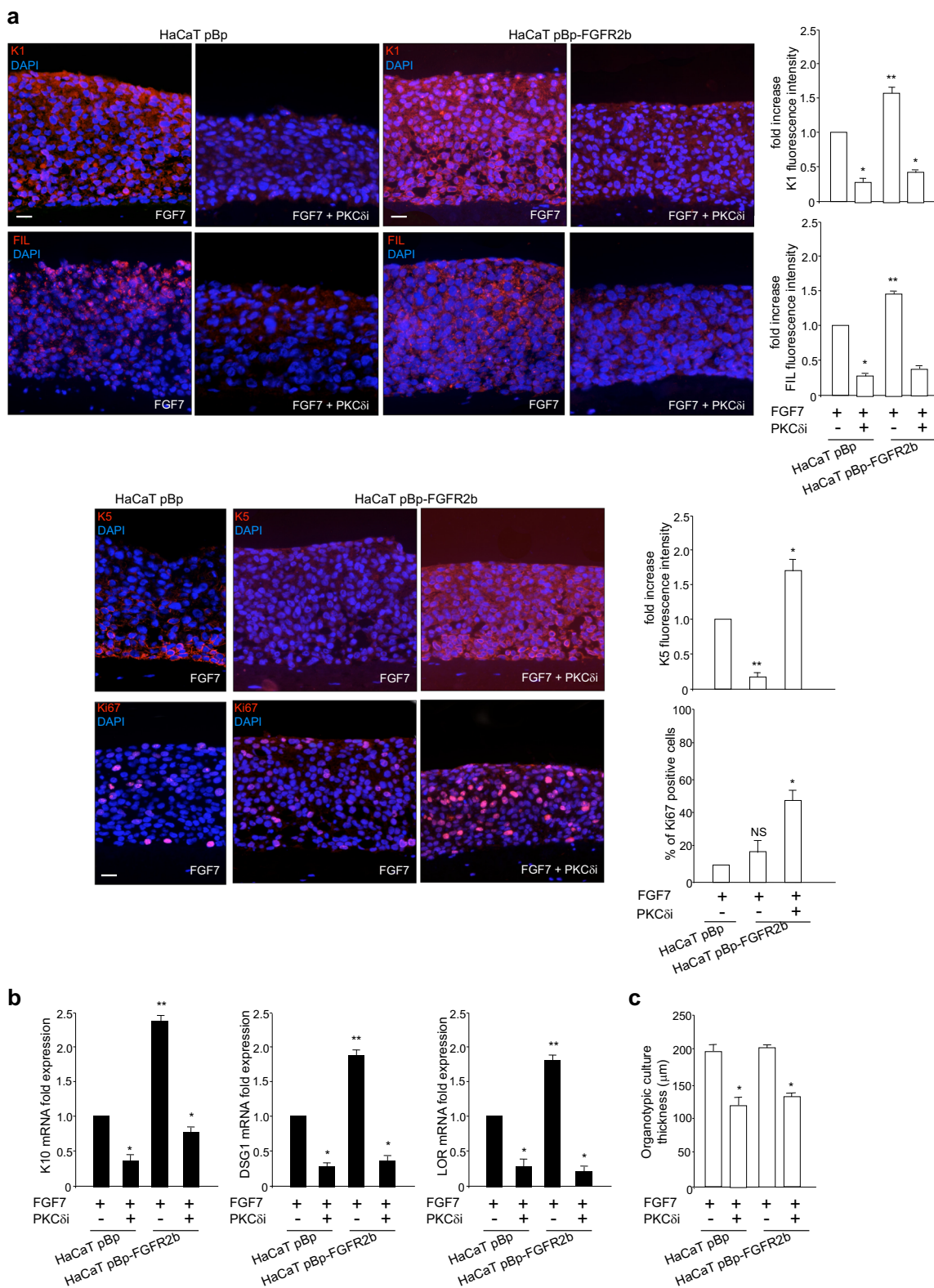


**Fig. 5** (See legend on next page.)

(see figure on previous page)

**Fig. 5 PKC $\delta$  signaling shut-off blocks the entire differentiation program and induces defective stratification in keratinocytes.** Organotypic skin equivalents of HaCaT pBp and pBp-FGFR2b clones, prepared as reported in Materials and methods section, were lifted to air–liquid interface in the presence or not of PKC $\delta$  inhibitor and finally stimulated with FGF7 as above. **a** Quantitative immunofluorescence analysis shows that K1 and FIL staining, visible in both HaCaT pBp and HaCaT pBp-FGFR2b rafts stimulated with FGF7, appears overall impaired by the presence of PKC $\delta$  inhibitor (upper panels). In addition, K5 signal, visible in the basal layer of pBp rafts, disappears in pBp-FGFR2b skin equivalents while it is recovered and distributed all over the pBp-FGFR2b rafts by the presence of PKC $\delta$  inhibitor (lower panels). Parallel evaluation of the nuclear proliferation marker Ki67 reveals the presence of few positive cells distributed in the basal layer and randomly throughout the suprabasal layers in pBp rafts and FGFR2b rafts stimulated with FGF7 (lower panels). In pBp-FGFR2b raft grown in the presence of PKC $\delta$ i, several cells intensely stained for Ki67 marker are visible in all the layers (lower panels). Quantitative analysis of the fluorescence intensity and of the percentage of Ki67 positive cells were performed as described in Materials and methods and results sections are expressed as fold increase respect to pBp values  $\pm$  SE. Student's *t* test was performed and significance levels have been defined as above: \**p* < 0.0001 vs the corresponding PKC $\delta$  inhibitor-untreated cells; NS and \*\**p* < 0.0001 vs the corresponding pBp cells. Bar: 25  $\mu$ m. **b** Real time RT-PCR analysis confirms that, in pBp and pBp-FGFR2b rafts stimulated with FGF7, the expression of K10, DSG1, and LOR is significantly repressed by PKC $\delta$  inhibitor. Results are expressed as mean values  $\pm$  SD. Student's *t* test was performed and significance levels have been defined as above: \**p* < 0.05 vs PKC $\delta$  inhibitor-untreated cells; \*\**p* < 0.05 vs the corresponding pBp cells. **c** Quantitative evaluation of the raft thickness shows that the layers of pBp and pBp-FGFR2b skin equivalents are significantly reduced by the presence of PKC $\delta$  inhibitor. Quantitative analysis of the raft thickness was expressed as  $\mu$ m mean  $\pm$  SD from three independent experiments. Student's *t* test was performed and significance levels have been defined as *p* < 0.05: \**p* < 0.0001 vs the corresponding PKC $\delta$  inhibitor-untreated cells

phenotypic features derived by PKC $\delta$  signaling shut-off indicate that the inhibition of this signaling pathway alone is sufficient to impair the balance between cell proliferation and differentiation controlled by FGFR2b. On the other hand, we can not exclude the contribution of the epidermal growth factor receptor (EGFR) in such increased cell proliferation: in fact, the antagonistic role of FGFR2b and EGFR in epithelial cells has been previously described by our group<sup>50</sup>. While FGFR2b is up-regulated during the shift from the basal to the suprabasal layers, EGFR mainly displays a basal distribution and its ligand-dependent activation triggers cell proliferation. In addition, it has been also proposed that FGF7/KGF treatment may induce endogenous synthesis of the EGFR ligand TGF $\alpha$ .<sup>51</sup> In any case, these results are in agreement with the widely described role of PKC $\delta$  as tumor suppressor, which is down-regulated in squamous cell carcinomas (SCCs)<sup>52,53</sup>.

Concerning the molecular effectors acting downstream PKC isoforms, our results showed that, in agreement with previous reports<sup>28,29,36</sup>, PKC $\delta$  and PKC $\alpha$  isoforms act via the induction of the downstream transcription factors KLF4 and DLX3, respectively. In fact, the expression of both KLF4 and DLX3 was clearly induced in response to FGF7, particularly in rafts or cell cultures overexpressing FGFR2b. Interestingly, in cultures grown at different cell densities to mimic the various steps of differentiation, we found that KLF4 up-regulation was mainly appreciable in confluent cells, while DLX3 induction was detectable only in post-confluent cultures. These sequential trends of induction could reflect the progressive involvement of their upstream inductors PKC $\delta$  and PKC $\alpha$  in the distinct stages (early and late, respectively) of differentiation.

Finally, we also decided to compare the modulation of KLF4 and DLX3 with that previously described for p63

and induced by FGFR2b signaling<sup>16,41</sup>. In fact, the FGFR2b/p63 crosstalk appears to be central in the homeostatic balance between keratinocyte proliferation and differentiation and its impairment, due to out-of-context appearance of FGFR2c, leads to loss of the differentiated phenotype and acquisition of tumorigenic features<sup>41</sup>. For this reason, to identify the molecular players contributing to the regulation of this crosstalk seems to represent a very urgent and important goal. Indeed, both KLF4 and DLX3 have been proposed to be involved in negative loops with p63:<sup>48,49</sup> consistent with these assumptions, we observed that they displayed opposite modulations compared to p63. Interestingly, the up-regulation of KLF4 appeared more appreciable in confluent cells, the same culture condition in which the down-regulation of p63 was more evident: this simultaneous detection of p63 down-regulation and KLF4 induction mainly in confluent cells strongly suggests that they take place in the same step of the differentiation program, and possibly during the shift between the basal to the suprabasal layer. These observations, together with the recent evidence of a possible direct role of PKC $\delta$  in p63 down-regulation<sup>54</sup>, allowed us to speculate that the down-regulation of p63 could represent the molecular mechanism through which FGFR2b and its downstream PKC $\delta$  signaling could induce the up-regulation of KLF4 and consequently the onset of keratinocyte differentiation.

## Materials and methods

### Cells and treatments

The human keratinocyte cell line HaCaT<sup>40</sup>, stably overexpressing FGFR2b (pBp-FGFR2b) or the empty vector (pBp) and generated as previously described<sup>6</sup>, were cultured in Dulbecco's modified Eagle's medium (DMEM), supplemented with 10% fetal bovine serum

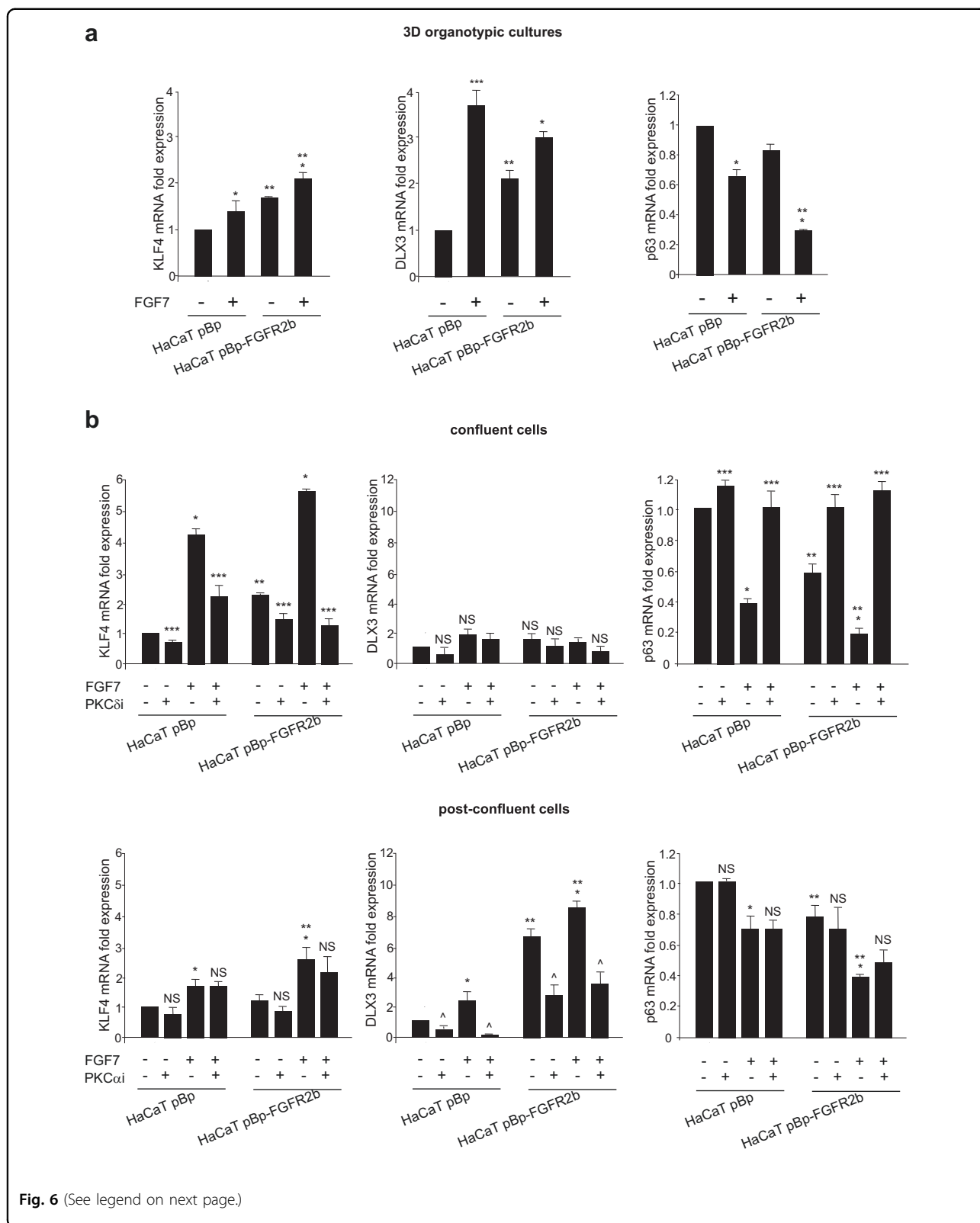


**Fig. 6** (See legend on next page.)

(see figure on previous page)

**Fig. 6 PKC $\delta$  and PKC $\alpha$  signaling are responsible for FGF7-mediated sequential induction of KLF4 and DLX3, respectively.** **a** Organotypic skin equivalents of HaCaT pBp and pBp-FGFR2b clones, prepared as reported in Materials and methods section, were grown in complete medium and left untreated or stimulated with FGF7 as above. Real time RT-PCR analysis shows a significant increase of both KLF4 and DLX3 expression upon FGF7 stimulation, while p63 displays an opposite trend. **b** HaCaT pBp and HaCaT pBp-FGFR2b cells were grown up to confluence or post-confluence in the presence or not of PKC $\delta$  and PKC $\alpha$  inhibitors, respectively, and stimulated with FGF7 as above. Real time RT-PCR analysis shows that KLF4 up-regulation is mainly appreciable in confluent clones, while DLX3 induction is detectable only in post-confluent cultures. The increased expression of KLF4 in confluent cells and that of DLX3 in post-confluent cultures are significantly dampened by PKC $\delta$ i and PKC $\alpha$ i, respectively. Similarly to KLF4, p63 down-modulation in response to FGF7 is more evident in confluent cells and it appears impaired only by PKC $\delta$ i. Results are expressed as mean values  $\pm$  SD. Student's *t* test was performed and significance levels have been defined as above: **a** \**p* < 0.05 and \*\*\**p* < 0.001 vs the corresponding FGF7-unstimulated cells; \*\**p* < 0.05 vs the corresponding pBp cells; **b** NS and \**p* < 0.05 vs the corresponding FGF7-unstimulated cells; NS and \*\**p* < 0.05 vs the corresponding pBp cells; NS and \*\*\**p* < 0.05 vs the corresponding PKC $\delta$  inhibitor-untreated cells; NS and  $\wedge$ *p* < 0.005 vs the corresponding PKC $\alpha$  inhibitor-untreated cells

(FBS) plus antibiotics. Primary cultures of human fibroblasts derived from healthy skin (HFs) were obtained from patients attending the Dermatology Unit of the Sant'Andrea Hospital of Rome; all patients were extensively informed and their consent for the investigation was given and collected in written form in accordance with guidelines approved by the management of the Sant'Andrea Hospital. HFs were isolated and cultured as previously described<sup>55</sup>.

For growth factors stimulation, cells were left untreated or incubated with FGF7 (Upstate Biotechnology, Lake Placid, NY, USA, 01–118) 100 ng/ml for 24 or 48 h at 37 °C. To inhibit AKT or MEK1/2 or PKC $\delta$  or PKC $\alpha$  cells were respectively incubated with the specific AKT inhibitor 1L-6-hydroxy-methyl-chiro-inositol 2-(R)-2-O-methyl-3-O-octadecylcarbonate (1  $\mu$ M; Calbiochem, Nottingham, UK, 124005) or with the specific MEK1/2 inhibitor PD0325901 (1  $\mu$ M; Sigma-Aldrich, Saint Louis, MO, USA, PZ0162) or with the specific PKC $\delta$  inhibitor rottlerin (5  $\mu$ M; Calbiochem, 557370) or with the specific PKC $\alpha$  inhibitor Go6976 (3  $\mu$ M; Calbiochem, 365250) for 1 h at 37 °C before treatment with FGF7 in the presence of each inhibitor.

For RNA interference and PKC $\delta$  or PKC $\alpha$  silencing, cells were transfected with PKC $\delta$  small interfering RNA (PKC $\delta$  siRNA) (Santa Cruz Biotechnology, Santa Cruz, CA, USA), or PKC $\alpha$  small interfering RNA (PKC $\alpha$  siRNA) (Santa Cruz Biotechnology), or with an unrelated siRNA as a control (control siRNA), using Lipofectamine 2000 Transfection Reagent (Invitrogen, Carlsbad, CA, USA) according to the manufacturer's protocol.

### Organotypic cultures

For three-dimensional (3D) organotypic cultures, collagen rafts were prepared adding 5 mg/ml rat tail type I collagen (Corning, Lowell, MA, USA) to DMEM and Reconstitution buffer (8:1:1) as previously described<sup>56</sup>. HFs (1  $\times$  10<sup>6</sup>) were added to 2 ml of the collagen mixture in polycarbonate micron inserts (23 mm diameter, pore size 0.3  $\mu$ m; Corning) in 6-deep well plates (Corning). The

mixture was left to polymerize for 30 min at 37 °C. After 24 h 2  $\times$  10<sup>5</sup> HaCaT pBp or pBp-FGFR2b cells were seeded on the collagen gel and left to grow for a week in complete medium added in both the top and the bottom wells. Then, the organotypic cultures were lifted to the air–liquid interface and cultured for further two weeks in complete medium added or not with the specific PKC $\delta$  inhibitor rottlerin (5  $\mu$ M; Calbiochem, 557370). Then cultures were left untreated or stimulated with FGF7 (Upstate Biotechnology) 100 ng/ml for the last 4 days. Rafts were finally fixed in 10% formalin, embedded in paraffin and 4  $\mu$ m slices were obtained. To evaluate organotypic thickness slices were stained with hematoxylin and eosin using standard procedures then bright field images were taken with an Axiocam ICc 5 (Zeiss, Oberkochen, Germany) connected with an Axioplan 100 microscope (Zeiss). The organotypic culture thickness was measured using the Axiovision software (Zeiss) and expressed as mean  $\mu$ m  $\pm$  standard deviation (SD). Student's *t* test was performed and significance levels have been defined as *p* < 0.05.

### Immunofluorescence

HaCaT clones, grown on coverslips, were fixed with 4% paraformaldehyde in PBS for 30 min at 25 °C followed by treatment with 0.1 M glycine for 20 min at 25 °C and with 0.1% Triton X-100 for additional 5 min at 25 °C to allow permeabilization. Cells were then incubated for 1 h at 25 °C with the following primary antibodies: rabbit polyclonal anti-K1 (1:50 in PBS, AF 87, Covance, Princeton, NJ, USA) or mouse monoclonal anti- $\beta$ 1 integrin (1:1000 in PBS; ST2–16, Santa Cruz Biotechnology). The primary antibodies were visualized using goat anti-rabbit IgG-Texas Red (1:200 in PBS; Jackson ImmunoResearch Laboratories, West Grove, PA, USA) or goat anti-mouse IgG-Alexa Fluor 488 (1:200 in PBS; Life Technologies, Carlsbad, CA, USA) antibodies for 30 min at 25 °C. Nuclei were stained with DAPI (1:1000 in PBS; Sigma). Coverslips were finally mounted with mowiol (Sigma) for observation.

Organotypic raft sections, obtained as above, were deparaffinized in xylene and re-hydrated through graded ethanols to PBS, pH 7.4. Antigen retrieval was achieved by heating sections in target retrieval solution low pH (Dako, Carpinteria, CA, USA) for 15 min at 97 °C. Sections were then washed with PBS and blocked using 10% bovine calf serum and 0.2% Triton X-100 for 30 min at 25 °C before staining with rabbit polyclonal anti-K1 (1:500 in PBS, AF 87, Covance), mouse monoclonal anti-filaggrin (1:1000 in PBS, 15C10, Monosan Sanbio, Uden, The Netherlands), rabbit polyclonal anti-cytokeratin 5 (1:400 in PBS, Abcam, Cambridge, UK) or mouse monoclonal anti-Ki67 (1:100 in PBS, MIB-1, Dako) antibodies for 1 h in a humidified chamber. The primary antibodies were visualized using goat anti-mouse IgG-Texas Red (1:200 in PBS; Jackson ImmunoResearch Laboratories) or goat anti-rabbit IgG-Texas Red (1:200 in PBS; Jackson ImmunoResearch Laboratories) antibodies for 30 min at 25 °C. Nuclei were stained with DAPI (1:1000 in PBS; Sigma). Sections were permanently mounted under a coverslip. Fluorescence signals were analyzed by conventional fluorescence or by scanning cells in a series of sequential sections with an ApoTome System (Zeiss) connected with an Axiovert 200 inverted microscope (Zeiss); image analysis was performed by the Axiovision software (Zeiss) and images were obtained by 3D reconstruction of the total number of the serial optical sections. Quantitative analysis of the fluorescence intensity was performed by the Axiovision software (Zeiss), analyzing 10 different fields randomly taken from three independent experiments. Quantitative analysis of the percentage of Ki67 positive cells was assessed counting for each sample a total of 50 cells, randomly observed in 10 microscopic fields from three different experiments. Results are shown as means  $\pm$  standard error (SE). Student's *t* test was performed and significance levels have been defined as  $p < 0.05$ .

#### Western blot analysis

Cells were lysed in a buffer containing 50 mM HEPES, pH 7.5, 150 mM NaCl, 1% glycerol, 1% Triton X-100, 1.5 mM MgCl<sub>2</sub>, 5 mM EGTA, supplemented with protease inhibitors (10  $\mu$ g/ml aprotinin, 1 mM PMSF, 10  $\mu$ g/ml leupeptin), and phosphatase inhibitors (1 mM sodium orthovanadate, 20 mM sodium pyrophosphate, 0.5 M NaF). A range between 20 and 50  $\mu$ g of total protein was resolved under reducing conditions by 8 or 12% SDS-PAGE and transferred to reinforced nitrocellulose (BA-S 83, Schleider and Schuell, Keene, NH, USA). The membranes were blocked with 5% nonfat dry milk in PBS 0.1% Tween 20 and incubated with anti-DSG1 (27B2, Life Technologies), anti- $\beta$ 1 integrin (ST2-16, Santa Cruz Biotechnology), anti-involucrin (SY5, Abcam), anti-filaggrin (15C10, Monosan), anti-p-PKC $\alpha$  (Ser657, Abcam) monoclonal antibody or with anti-K1 (AF 87,

Covance), anti-Bek (C-17, Santa Cruz Biotechnology), anti-loricrin (Covance), anti-p-PKC $\delta$  (Ser645, Santa Cruz Biotechnology) polyclonal antibodies, all followed by enhanced chemiluminescence detection (ECL, Amersham, Arlington Heights, IL, USA). The membranes were rehydrated by being washed in PBS-Tween 20, stripped with 100 mM mercaptoethanol and 2% SDS for 30 min at 55 °C, and probed again with anti-PKC $\delta$  (C-20, Santa Cruz Biotechnology) polyclonal antibodies, anti-PKC $\alpha$  monoclonal antibody (Y124, Abcam) or with anti- $\beta$ -ACTIN (AC-15, Sigma) monoclonal antibody or anti- $\alpha$ -TUBULIN (2148S, Cell Signaling) polyclonal antibodies to estimate the protein equal loading. Densitometric analysis was performed using Quantity One Program (Bio-Rad Laboratories, Hercules, CA, USA). Results from three different experiments were normalized and expressed as fold increase respect to the control value. Values from a representative of three independent experiments were reported in each figure.

#### Primers

Oligonucleotide primers necessary for target genes and the housekeeping gene were chosen utilizing the online tool Primer-BLAST and purchased from Invitrogen. Primers list and characteristics are reported in Supplementary Table S1. For *p63* target gene, the reported primers were designed to recognize both  $\Delta$ Np63 and TAp63  $\alpha$  and  $\beta$  isoforms. For each primer pair, we performed no-template control and no-reverse-transcriptase control (RT negative) assays, which produced negligible signals.

#### RNA extraction and cDNA synthesis

Organotypic cultures were deparaffinized and RNA was extracted using the TRIzol method (Invitrogen) according to manufacturer's instructions and eluted with 0.1% diethylpyrocarbonate (DEPC)-treated water. Each sample was treated with DNAase I (Invitrogen). Total RNA concentration was quantitated by spectrophotometry; 1  $\mu$ g of total RNA was used to reverse transcription using iScript<sup>TM</sup> cDNA synthesis kit (Bio-Rad) according to manufacturer's instructions.

#### PCR amplification and real time quantitation

Real time RT-PCR was performed using the iCycler Real Time Detection System (iQ5 Bio-Rad) with optimized PCR conditions. The reaction was carried out in 96-well plate using iQ SYBR Green Supermix (Bio-Rad) adding forward and reverse primers for each gene and 1  $\mu$ l of diluted template cDNA to a final reaction volume of 15  $\mu$ l. All assays included a negative control and were replicated three times. The thermal cycling program was performed as described<sup>6</sup>. Real time quantitation was performed with the help of the iCycler IQ optical system software version 3.0a (Bio-Rad), according to the manufacturer's manual.

Results are reported as mean  $\pm$  SD from three different experiments in triplicate. Student's *t* test was performed and significance levels have been defined as  $p < 0.05$ .

### Statistical analysis

Data were statistically analyzed with unpaired two-tailed Student's *t* test. Differences were considered significant at the level of  $p < 0.05$ . Statistical analysis was performed by using Microsoft Excel 2016 Spreadsheet Software (Microsoft® Software; Redmond, Washington, United States).

### Acknowledgements

This work was partially supported by grants from MIUR and from AIRC - Associazione Italiana per la Ricerca sul Cancro, Italy (Grant number: IG 15858).

### Conflict of interest

The authors declare that they have no conflict of interest.

### Publisher's note

Springer Nature remains neutral with regard to jurisdictional claims in published maps and institutional affiliations.

**Supplementary Information** accompanies this paper at (<https://doi.org/10.1038/s41419-018-0509-x>).

Received: 28 November 2017 Revised: 16 February 2018 Accepted: 15 March 2018

Published online: 11 May 2018

### References

- Turner, N. & Grose, R. Fibroblast growth factor signalling: from development to cancer. *Nat. Rev. Cancer* **10**, 116–129 (2010).
- Goetz, R. & Mohammadi, M. Exploring mechanisms of FGF signalling through the lens of structural biology. *Nat. Rev. Mol. Cell. Biol.* **14**, 166–180 (2013).
- Haugsten, E. M., Wiedlocha, A., Olsnes, S. & Wesche, J. Roles of fibroblast growth factor receptors in carcinogenesis. *Mol. Cancer Res.* **8**, 1439–1452 (2010).
- Brooks, A. N., Kilgour, E. & Smith, P. D. Molecular pathways: fibroblast growth factor signaling: a new therapeutic opportunity in cancer. *Clin. Cancer Res.* **18**, 1855–1862 (2012).
- Ranieri, D., Belleudi, F., Magenta, A. & Torrisi, M. R. HPV16 E5 expression induces switching from FGFR2b to FGFR2c and epithelial-mesenchymal transition. *Int. J. Cancer* **137**, 61–72 (2015).
- Ranieri, D. et al. Expression of the FGFR2 mesenchymal splicing variant in epithelial cells drives epithelial-mesenchymal transition. *Oncotarget* **7**, 5440–5460 (2016).
- Oltean, S. et al. Alternative inclusion of fibroblast growth factor receptor 2 exon IIIc in Dunning prostate tumors reveals unexpected epithelial mesenchymal plasticity. *Proc. Natl Acad. Sci. USA* **103**, 14116–14121 (2006).
- Zhao, Q. et al. Tumor-specific isoform switch of the fibroblast growth factor receptor 2 underlies the mesenchymal and malignant phenotypes of clear cell renal cell carcinomas. *Clin. Cancer Res.* **19**, 2460–2472 (2013).
- Feng, S., Wang, F., Matsubara, A., Kan, M. & McKeenan, W. L. Fibroblast growth factor receptor 2 limits and receptor 1 accelerates tumorigenicity of prostate epithelial cells. *Cancer Res.* **58**, 1509–1514 (1997).
- Zhang, Y. et al. Growth inhibition by keratinocyte growth factor receptor of human salivary adenocarcinoma cells through induction of differentiation and apoptosis. *Proc. Natl Acad. Sci. USA* **98**, 11336–11340 (2001).
- Petiot, A. et al. A crucial role for Fgfr2-IIIb signalling in epidermal development and hair follicle patterning. *Development* **130**, 5493–5501 (2003).
- Grose, R. et al. The role of fibroblast growth factor receptor 2b in skin homeostasis and cancer development. *EMBO J.* **26**, 1268–1278 (2007).
- Yang, J. et al. Fibroblast growth factor receptors 1 and 2 in keratinocytes control the epidermal barrier and cutaneous homeostasis. *J. Cell Biol.* **188**, 935–952 (2010).
- Capone, A. et al. Up-modulation of the expression of functional keratinocyte growth factor receptors induced by high cell density in the human keratinocyte HaCaT cell line. *Cell Growth Differ.* **11**, 607–614 (2000).
- Belleudi, F., Purpura, V. & Torrisi, M. R. The receptor tyrosine kinase FGFR2b/KGFR controls early differentiation of human keratinocytes. *PLoS ONE* **6**, e24194 (2011).
- Purpura, V., Belleudi, F., Caputo, S. & Torrisi, M. R. HPV16 E5 and KGFR/FGFR2b interplay in differentiating epithelial cells. *Oncotarget* **4**, 192–205 (2013).
- Candi, E. et al. p63 in epithelial development. *Cell. Mol. Life. Sci.* **65**, 3126–3133 (2008).
- Hines, M. D. & Allen-Hoffmann, B. L. Keratinocyte growth factor inhibits cross-linked envelope formation and nucleosomal fragmentation in cultured human keratinocytes. *J. Biol. Chem.* **271**, 6245–6251 (1996).
- Andreadis, S. T., Hamoen, K. E., Yarmush, M. L. & Morgan, J. R. Keratinocyte growth factor induces hyperproliferation and delays differentiation in a skin equivalent model system. *FASEB J.* **15**, 898–906 (2001).
- Marchese, C. et al. Fibroblast growth factor 10 induces proliferation and differentiation of human primary cultured keratinocytes. *J. Invest. Dermatol.* **116**, 623–628 (2001).
- Kim, H. J. et al. The protein kinase C pathway plays a central role in the fibroblast growth factor-stimulated expression and transactivation activity of Runx2. *J. Biol. Chem.* **278**, 319–326 (2003).
- Miraoui, H. et al. Fibroblast growth factor receptor 2 promotes osteogenic differentiation in mesenchymal cells via ERK1/2 and protein kinase C signaling. *J. Biol. Chem.* **284**, 4897–4904 (2009).
- Breitkreutz, D., Braiman-Wiksmann, L., Daum, N., Denning, M. F. & Tennenbaum, T. Protein kinase C family: on the crossroads of cell signaling in skin and tumor epithelium. *J. Cancer Res. Clin. Oncol.* **133**, 793–808 (2007).
- Efimova, T. & Eckert, R. L. Regulation of human involucrin promoter activity by novel protein kinase C isoforms. *J. Biol. Chem.* **275**, 1601–1607 (2000).
- Deucher, A., Efimova, T. & Eckert, R. L. Calcium-dependent involucrin expression is inversely regulated by protein kinase C (PKC)alpha and PKCdelta. *J. Biol. Chem.* **277**, 17032–17040 (2002).
- Szegedi, A. et al. Protein kinase C isoenzymes differentially regulate the differentiation-dependent expression of adhesion molecules in human epidermal keratinocytes. *Exp. Dermatol.* **18**, 122–129 (2009).
- Adhikary, G., Chew, Y. C., Reece, E. A. & Eckert, R. L. PKC-delta and -eta, MEK-1, MEK-3, and p38-delta are essential mediators of the response of normal human epidermal keratinocytes to differentiating agents. *J. Invest. Dermatol.* **130**, 2017–2030 (2010).
- Chew, Y. C., Adhikary, G., Wilson, G. M., Reece, E. A. & Eckert, R. L. Protein kinase C (PKC) delta suppresses keratinocyte proliferation by increasing p21 (Cip1) level by a KLF4 transcription factor-dependent mechanism. *J. Biol. Chem.* **286**, 28772–28782 (2011).
- Chew, Y. C., Adhikary, G., Xu, W., Wilson, G. M. & Eckert, R. L. Protein kinase C  $\delta$  increases Kruppel-like factor 4 protein, which drives involucrin gene transcription in differentiating keratinocytes. *J. Biol. Chem.* **288**, 17759–17768 (2013).
- Alt, A., Gartsbein, M., Ohba, M., Kuroki, T. & Tennenbaum, T. Differential regulation of alpha6beta4 integrin by PKC isoforms in murine skin keratinocytes. *Biochem. Biophys. Res. Commun.* **314**, 17–23 (2004).
- Alt, A. et al. Protein kinase Cdelta-mediated phosphorylation of alpha6beta4 is associated with reduced integrin localization to the hemidesmosome and decreased keratinocyte attachment. *Cancer Res.* **61**, 4591–4598 (2001).
- Candi, E., Schmidt, R. & Melino, G. The cornified envelope: a model of cell death in the skin. *Nat. Rev. Mol. Cell Biol.* **6**, 328–340 (2005).
- Dlugosz, A. A. et al. Alterations in murine keratinocyte differentiation induced by activated rasHa genes are mediated by protein kinase C-alpha. *Cancer Res.* **54**, 6413–6420 (1994).
- Stanwell, C. et al. Staurosporine induces a sequential program of mouse keratinocyte terminal differentiation through activation of PKC isozymes. *J. Invest. Dermatol.* **106**, 482–489 (1996).
- Jerome-Morais, A., Rahn, H. R., Tibudan, S. S. & Denning, M. F. Role for protein kinase C-alpha in keratinocyte growth arrest. *J. Invest. Dermatol.* **129**, 2365–2375 (2009).
- Palazzo, E. et al. A novel DLX3-PKC integrated signaling network drives keratinocyte differentiation. *Cell Death. Differ.* **24**, 717–730 (2017).

37. Morasso, M., Markova, N. G. & Sargent, T. D. Regulation of epidermal differentiation by a Distal-less homeodomain gene. *J. Cell Biol.* **135**, 1879–1887 (1996).
38. Hwang, J. et al. Epidermal ablation of Dlx3 is linked to IL-17-associated skin inflammation. *Proc. Natl Acad. Sci. USA* **108**, 11566–11571 (2011).
39. Palazzo, E. et al. The homeoprotein DLX3 and tumor suppressor p53 co-regulate cell cycle progression and squamous tumor growth. *Oncogene* **35**, 3114–3124 (2016).
40. Boukamp, P. et al. Normal keratinization in a spontaneously immortalized aneuploid human keratinocyte cell line. *J. Cell Biol.* **106**, 761–771 (1988).
41. Ranieri, D., Rosato, B., Nanni, M., Belleudi, F. & Torrisi, M. R. Expression of the FGFR2c mesenchymal splicing variant in human keratinocytes inhibits differentiation and promotes invasion. *Mol. Carcinog.* **57**, 272–283 (2018).
42. Levy, L., Broad, S., Diekmann, D., Evans, R. D. & Watt, F. M. beta1 integrins regulate keratinocyte adhesion and differentiation by distinct mechanisms. *Mol. Biol. Cell* **11**, 453–466 (2000).
43. Nanni, M., Ranieri, D., Raffa, S., Torrisi, M. R. & Belleudi, F. Interplay between FGFR2b-induced autophagy and phagocytosis: role of PLCγ –mediated signaling. *J. Cell. Mol. Med.* **22**, 668–683 (2017).
44. Stempka, L. et al. Requirements of protein kinase delta for catalytic function. Role of glutamic acid 500 and autophosphorylation on serine 643. *J. Biol. Chem.* **274**, 8886–8892 (1999).
45. Bornancin, F. & Parker, P. J. Phosphorylation of threonine 638 critically controls the dephosphorylation and inactivation of protein kinase Cα. *Curr. Biol.* **6**, 1114–1123 (1996).
46. Belleudi, F., Purpura, V., Caputo, S. & Torrisi, M. R. FGF7/KGF regulates autophagy in keratinocytes: A novel dual role in the induction of both assembly and turnover of autophagosomes. *Autophagy* **10**, 803–821 (2014).
47. Radoja, N. et al. Homeobox gene Dlx3 is regulated by p63 during ectoderm development: relevance in the pathogenesis of ectodermal dysplasias. *Development* **134**, 13–18 (2007).
48. Di Costanzo, A. et al. Homeodomain protein Dlx3 induces phosphorylation-dependent p63 degradation. *Cell Cycle* **8**, 1185–1195 (2009).
49. Cordani, N. et al. Mutant p53 subverts p63 control over KLF4 expression in keratinocytes. *Oncogene* **30**, 922–932 (2011).
50. Belleudi, F. et al. Endocytic pathways and biological effects induced by UVB-dependent or ligand-dependent activation of the keratinocyte growth factor receptor. *FASEB J.* **20**, 395–397 (2006).
51. Dlugosz, A. A. et al. Keratinocyte growth factor receptor ligands induce transforming growth factor alpha expression and activate the epidermal growth factor receptor signaling pathway in cultured epidermal keratinocytes. *Cell Growth Differ.* **5**, 1283–1292 (1994).
52. D'Costa, A. M. et al. The proapoptotic tumor suppressor protein kinase C-delta is lost in human squamous cell carcinomas. *Oncogene* **25**, 378–386 (2006).
53. Yadav, V., Yanez, N. C., Fenton, S. E. & Denning, M. F. Loss of protein kinase C delta gene expression in human squamous cell carcinomas: a laser capture microdissection study. *Am. J. Pathol.* **176**, 1091–1096 (2010).
54. Zhang, D. et al. PKC-δ attenuates the cancer stem cell among squamous cell carcinoma cells through down-regulating p63. *Pathol. Res. Pract.* **213**, 1119–1124 (2017).
55. Raffa, S. et al. Cholesteatoma-associated fibroblasts modulate epithelial growth and differentiation through KGF/FGF7 secretion. *Histochem. Cell Biol.* **138**, 251–269 (2012).
56. Anacker, D. & Moody, C. Generation of organotypic raft cultures from primary human keratinocytes. *J. Vis. Exp.* **60**, e3668 (2012).